

Supplementary Material

1
2
3
4
5
6
7
8
9
10
11
12
13
14
15
16
17
18
19
20
21

Table S1: Paleontological age constraints of the Cretaceous terrestrial deposits in the Asian interior basins

Table S2: Stratigraphic compilation of the climate-sensitive sediments with special emphasis on desert (eolian dune) deposits cited in **Figure 3**.

Supplementary Methods: Paleoposition and Age constraints for the eolian sandstone formations in the Asian interior basins

Figure S1: Lithostratigraphic column, paleowind direction data, and magnetic polarity sequence of the eolian sandstone deposits (Jiaguan Formation) in Sichuan Basin, south China

Figure S2: Lithostratigraphic column, paleowind direction data, and magnetic polarity sequence of the eolian sandstone deposits (Phu Thok Formation) in the Khorat Basin, northeast Thailand

Supplementary References

22 **Table S1:** Paleontological age constraints of the Cretaceous terrestrial deposits in the Asian
 23 interior basins based on the fossil assemblages of ostracods, charophytes, pollen and spores
 24 (modified after, Li, 1982; Racey et al., 1996; Hao et al., 2000; Khand et al., 2000; Meesok,
 25 2000; Chen et al., 2006; Sha, 2007; Hasegawa et al., 2010).

26

27 **Gobi Basin**

Formation	Lithology	Fossil assemblage	Age
Tsagantsav Fm	Reddish brown to whitish grey, conglomerate and sandstone, reddish brown mudstone, calcretes, basalts	Ostracodes: <i>Cypridea unicastata</i> Plants: <i>Baiera manchurica</i> , <i>Cladophiledis onychiopsis</i> , <i>Nilssoniopteris denticulata</i>	Ber.–Brm.
Shinehudag Fm	Greenish grey to whitish grey, siltstone & mudstone	Ostracodes: <i>Cypridea fasciculata</i> Charophytes: <i>Aclistochara caii</i> , <i>Raskyella sp.</i> Pollen & Spores: <i>Cicatricosisporites australiensis</i> , <i>Densoisporites velatus</i> , <i>Pilosisporites trichopapilosus</i>	Brm?–Apt.
Khukhteeg Fm	Whitish grey to brown, conglomerate, sandstone, mudstone, & lignites	Ostracodes: <i>Cypridea acutituberculata</i> , <i>Tsetsenia mira</i> , <i>Trapeoidella khandae</i> , <i>Janinella tsaganensis</i> Charophytes: <i>Atopochara trivolvis</i> , <i>Mesochara voluta</i> , <i>M. tuzsoni</i> Pollen & Spores: <i>Foraminisporites assemmetricus</i> , <i>Alisporites elongatus</i> , <i>Abiespollenites sp.</i>	Alb.
Bayanshiree Fm	Reddish brown to whitish grey, conglomerate, sandstone, mudstone, & calcretes	Ostracodes: <i>Lycocypris baishintsavica</i> , Charophytes: <i>Atopochara multivolvis</i> , <i>Caucasuella gulistanica</i>	Cen.–San.
Djadokhta Fm	Reddish to reddish brown, eolian sandstone & mudstone	Ostracodes: <i>Gobiocypris tugrigensis</i>	e. Camp.
Barungoyot Fm	Reddish to reddish brown, eolian sandstone & mudstone	Ostracodes: <i>Talicypridea abdarantica</i>	l. Camp.
Nemegt Fm	Reddish brown to whitish grey, conglomerate, sandstone, mudstone, & calcretes	Ostracodes: <i>Talicypridea reticulata</i> , <i>Mongolocypis distributa</i> Charophytes: <i>Mongololiachara mesochara</i>	e. Maas.
Dzunmod Fm	Reddish brown to whitish grey, eolian sandstone, mudstone, & calcretes	no fossils	m. Maas.

28

29 **Ordos Basin**

Formation	Lithology	Fossil assemblage	Age
Luohe Fm	Red to purple, fine- to medium-grained, eolian sandstone	Ostracodes: <i>Darwinula contracta</i> Vertebrates: <i>Lycoptera sp.</i>	Ber.–Vlg.
Huanhe Fm (Huachi Fm)	Yellowish-green to reddish-purple, fine-grained sandstone, siltstone, & mudstone	Ostracodes: <i>Cypridea unicastata</i> , <i>C. koskulensis</i> , <i>Rhinocypris cirrita</i> Dinosaurs: <i>Psittacosaurus sp.</i>	Vlg.
Luohangdong Fm	Red to purple, fine- to medium-grained, eolian sandstone	Ostracodes: <i>Cypridea vitimensis</i> , <i>C. consulta</i> , <i>C. koskulensis</i> , <i>Clinocypris scolida</i> , <i>Rhinocypris cirrita</i> , <i>Lycocypris infantilis</i> , <i>Darwinula simplicus</i> , <i>Rhinocypris foveata</i> , <i>Djungarica stolidia</i> Dinosaurs: <i>Psittacosaurus youngi</i>	Vlg.–Hau.
Jingchuang Fm	Yellowish-green to reddish-purple, fine-grained sandstone, siltstone, & mudstone	Ostracodes: <i>Cypridea unicastata</i> , <i>C. yumenensis</i> , <i>C. justa</i> , <i>C. koskulensis</i> , <i>C. consulta</i> , <i>C. subrostrata</i> , <i>Pseudocypridina globra</i> , <i>Clinocypris scolida</i> , <i>Lycocypris infantilis</i> , <i>Jungarica stolidia</i> , <i>Rhinocypris foveata</i> , <i>R. cirrita</i>	Hau.–Brm.

		Pollen & Spores: <i>Cicatricosis porites</i> , <i>Densois porites</i> , <i>Piceae pollenites</i> Dinosaurs: <i>Psittacosaurus youngi</i>	
Lamawan Fm	Yellowish-grey to whitish-grey, medium- to coarse-grained sandstone, mudstone, & coals	Plants: <i>Elatocladus manchuricus</i> , <i>E. obtusifolia</i> , <i>Brachyphyllum japonicum</i> , <i>Sphenolepidium sp.</i> , <i>Coniopteris onychioides</i> , <i>Czekanowskia rigida</i> , <i>Podozamites lanoeolatus</i> , <i>Stenorachis bulunensis</i>	Brm.–Apt.
Tegaimiao Fm	Red to orange, fine- to medium-grained, eolian sandstone	Dinosaurs: <i>Protoceratops sp.</i>	San.–Camp.

30

31 Tarim Basin

Formation	Lithology	Fossil assemblage	Age
Kezilesu Gp	Red to purple, conglomerate, sandstone, & sandy mudstone	Ostracodes: <i>Darwinnela contracta</i> , <i>Cypridea koskulensis</i> , <i>Lycoperocypris circulata</i> , <i>Rhinocypris cirrita</i> , Charophytes: <i>Cicatricosisporites sp.</i> , <i>Crybelospprites sp.</i> Pollen & Spores: <i>Cicatricosis porites</i> , <i>Schizaeois certus</i> , <i>Dicheiropollis etrusus</i> , <i>Crybelospprites sp.</i> , <i>Clavatipollenites sp.</i> , <i>Liliacidites sp.</i>	Ber.–Brm.
Kumutake Fm	Red to orange, pebbly sandstone, sandstone, & mudstone	Ostracodes: <i>Talicypridea meliora</i> , <i>T. gemma</i> , <i>Cypridea cavernosa</i> , <i>C. rostrata</i> , <i>Ziziphocypris simakovi</i> , <i>Candoniella mordvilkoii</i>	Con.–Camp.
Subashi Fm	Whitish-grey to reddish, medium to coarse-grained sandstone, & mudstone	Ostracodes: <i>Cypridea mosuowanensi</i> , <i>Talicypridea amoena</i> , <i>T. gemma</i> , <i>T. retusa</i> Dinosaurs: <i>Tarbosaurus sp.</i> , <i>Nemegtosaurus pachi</i> , <i>Oolithes spherides</i> , <i>Mongolimys turfanensis</i> , <i>Shanshanosaurus huoyanshanensis</i>	Camp.–Maas.

32

33 Subei Basin

Formation	Lithology	Fossil assemblage	Age
Xihengshan Fm	Yellowish grey to purple, sandstone, mudstone, & coals	Ostracodes: <i>Cypridea sp.</i> Plants: <i>Gleichenites nipponensis</i> , <i>Brachyphyllum besum</i> , <i>Sphenopteris nitidula</i>	Ber.–Vlg.
Longwangshan Fm	Whitish grey to purple, andesite lava, & andesitic tuff breccia	no fossils	Vlg.
Dawangshan Fm	Purple to grey, andesitic tuff breccia	Plants: <i>Pagiophyllum sp.</i> , <i>Potozamites sp.</i> , <i>Otozamites sp.</i>	Hau.–Brm.
Gecun Fm	Reddish orange, greenish grey, sandstone, & mudstone	Charophytes: <i>Sphaerochara vertieillata</i> , <i>S. stontoni</i> , <i>Charites symmetrica</i> , <i>Flabellochara jurongica</i> Pollen & Spores: <i>Classopollis sp.</i> , <i>Cicatricosisporites sp.</i> Plants: <i>Frenelopsis sp.</i>	Apt.–Alb.
Pukou Fm	Reddish-purple to grey, pebbly sandstone	Ostracodes: <i>Cypridea sp.</i> , <i>Talicypridea sp.</i> , <i>Ziphocypris simakovi</i> Pollen & Spores: <i>Hizaeois porites</i> , <i>Welwitshia pites</i>	Cen.–Con.
Chishan Fm	Reddish-purple to greenish-grey, sandstone & mudstone	Ostracodes: <i>Cypridea cavernosa</i> , <i>Talicypridea sp.</i> , <i>Eucypris sp.</i> Plants: <i>Manica tholistoma</i>	San.–Maas.

34

35 Jiangnan Basin

Formation	Lithology	Fossil assemblage	Age
Wulong Fm	Reddish to yellowish-grey, conglomerate, sandstone,	Ostracodes: <i>Cypridea prognata</i> , <i>Mantelliana gigantea</i> , <i>Ziziphocypris simakovi</i> ,	Alb.

	mudstone	<i>Monosulcocypriis</i> sp. Charophytes: <i>Mesochara symmetrica</i> , <i>M. stantoni</i> , <i>Flabellochara hangzhouensis</i> , <i>Euaclistochara mundula</i> Pollen & Spores: <i>Cicatricosisporites apicanalis</i> , <i>C. tersus</i> , <i>C. dorogensis</i> , <i>C. minutaetritatus</i> , <i>Klukisporites variegatus</i> , <i>Toroisporis pseudodorogensis</i> , <i>Lygodiumsporites subsimplex</i> , <i>Schizaeois porites cretaceosm</i> <i>S. phaseolus</i> Plants: <i>Manica parceramosa</i>	
Luoqinghu Fm	Reddish-purple to grey, conglomerate, sandstone	Ostracodes: <i>Cypridea cavernosa</i>	Cen.–Tur.
Honghuatao Fm	Reddish to yellowish orange, fine-grained eolian sandstone	Ostracodes: <i>Cypridea cavernosa</i> , <i>Talicypridea amoena</i> , <i>T. longa</i> Charophytes: <i>Porochara anluensis</i>	Con.–San.
Paomagang Fm	Reddish to whitish grey, sandstone & mudstone	Ostracodes: <i>Cypridea cavernosa</i> , <i>C. nanxiongensis</i> , <i>C. tera</i> , <i>Talicypridea amoena</i> , <i>T. longa</i> , <i>T. chinensis</i> , <i>T. quadrata</i> Charophytes: <i>Latochara cylindrica</i> , <i>L. curtula</i> , <i>L. yunnanensis</i> , <i>Peckichara dangyangensis</i> , <i>Charites tenuis</i>	Camp.–Maas.

36

37 Sichuan Basin

Formation	Lithology	Fossil assemblage	Age
Tianmashan Fm	Reddish-purple conglomerate, sandstone, & mudstone	Ostracodes: <i>Deyangia lushanensis</i> , <i>D. postacuta</i> , <i>Cypridea</i> sp., <i>Jingguella obtusura</i> , <i>Lycocypris</i> sp., <i>Minheella</i> sp., <i>Ziziphocypris</i> sp., <i>Mongolianella</i> sp.	Ber.–Brm.
Jiaguan Fm	Reddish-purple, fine- to medium-grained, eolian sandstone	Ostracodes: <i>Cypridea angusticaudata</i> , <i>C. sichuanensis</i> , <i>C. yunnanensis</i> , <i>C. gunzulingensis</i> , <i>C. enodata</i> , <i>C. cf. ampullacea</i> , <i>C. concise</i> , <i>C. tera</i> , <i>C. cf. gibbosa</i> , <i>C. setina frorida</i> , <i>C. sentina acerata</i> , <i>C. setina bellatula</i> , <i>C. (Bisulcocypriidea)</i> sp., <i>C. (B.) chuxiongensis</i> , <i>C. (Morinina) monosulcata</i> , <i>Harbinia jingshanensis</i> , <i>Latonia (Monosulcocypriis) spp.</i> , <i>Sinocypris (Quadracypris) cf. favosa</i> , <i>Talicypridea (Cristocypridea) sp.</i> , <i>Ziziphocypris orbita</i> , <i>Z. acuta</i> , <i>Jinggunella</i> sp., <i>Kaitunia cuneata</i> , <i>Darwinnella</i> sp., <i>Timiriasevia</i> sp., <i>Lycocypris</i> sp., <i>Pinnocypridea</i> sp.	Apt.–Tur.
Guankou Fm	Red to purple, fine-grained sandstone, mudstone, gypsum	Ostracodes: <i>Cypridea gigantea</i> , <i>C. infidelis</i> , <i>Cristocypridea latiovata</i> , <i>C. chinensis</i> , <i>Sinocypris subfuningensis</i> , <i>Candona huangdianensis</i> , <i>C. qionglaiensis</i> , <i>Nonion sichuanensis</i> ,	Con.–Maas.

38

39 Simao Basin

Formation	Lithology	Fossil assemblage	Age
Jingxing Fm	Yellowish-grey to whitish-grey, sandstone, mudstone, & coals	Ostracodes: <i>Monosulcocypriis reticulata</i> , <i>Cypridea angusticaudata</i> , <i>Candona yunnanensis</i> , <i>Rhinocypris tuberculata</i> , <i>Limnocythere tumulosa</i>	Ber.–Brm.
Nanxin Fm	Red to purple, sandstone, & mudstone	Ostracodes: <i>Monosulcocypriis subovata</i> , <i>M. subelliptica</i> , <i>M. longa</i> , <i>M. gigantea</i> , <i>M. yunnanensis</i> , <i>M. ventricconvexa</i> , <i>M. reticulata</i> , <i>Ziziphocypris simakovi</i> , <i>Rhinocypris tuberculata</i> Charophytes: <i>Atopochara trivolvis</i> , <i>Nodoclavator puchanghensis</i>	Apt.–Alb.
Bashahe Fm	Reddish-purple, eolian sandstone and sandy mudstone	no fossils	Cen.–Tur.
Mankuanhe Fm	Red to purple, sandy	Ostracodes: <i>Eucypris anluensis</i> , <i>Cypridea</i>	Con.–Maas.

	mudstone, & mudstone	<i>zhengdongensis</i> , <i>C. cavernosa</i> , <i>Sinocypris zhengdongensis</i> , <i>S. reniformis</i> , <i>Talicypridea subparallela</i> , <i>T. xishuangbananensis</i> , <i>T. amoena</i> Charophytes: <i>Peckichara dongyangensis</i> , <i>Charites tenuisa</i>	
--	----------------------	--	--

40

41 Khorat Basin

Formation	Lithology	Fossil assemblage	Age
Phu Kradong Fm	Reddish brown, sandstone, siltstone, & mudstone	Pollen & Spores: <i>Cyathidites minor</i> , <i>Baculatisporites commaumensis</i> , <i>Corollina simplex</i>	E. Cretaceous
Phra Wihan Fm	Whitish-grey, conglomerate, sandstone, mudstone, & lignites	Pollen & Spores: <i>Cicatricosisporites augustus</i> , <i>Dicheiropollis etruscus</i> , <i>Corollina spp.</i> , <i>Araucariacites australis</i> , <i>Ischyosporites cf. variegatus</i> , <i>Gleichenidites senonicus</i> , <i>Laevigatosporites sp.</i> , <i>Perinopollenites elatoides</i> , <i>Callialasporites dampieri</i> , <i>Anaplanisporites dawsonensis</i> , <i>Apiculatisporites spp.</i> , <i>Osmundacidites wellmanii</i> , <i>Todisporites minor</i> , <i>Kraeuselisporites sp.</i> , <i>Concavissimisporites sp.</i>	Ber.–Brm.
Sao Khua Fm	Reddish brown, sandstone, siltstone, & mudstone	Pollen & Spores: <i>Vitreisporites cf. pallidus</i> , <i>Cicatricosisporites spp.</i> , <i>Cyathidites minor spp.</i> , <i>Ephedripites spp.</i> , <i>?Araucariacites australis</i>	E. Cretaceous
Phu Phan Fm	Whitish-grey, conglomerate, sandstone, mudstone	Pollen & Spores: <i>Corollina spp.</i> , <i>Cyathidites minor</i> , <i>?Todisporites sp.</i>	E. Cretaceous
Khok Kruat Fm	Reddish brown, sandstone, siltstone, & mudstone	Pollen & Spores: no data presented*	Apt.?
Maha Sarakhan Fm	Reddish, sandstone, siltstone, salts, gypsums, & anhydrites	Pollen & Spores: no data presented*	Alb.?–Cen.?
Phu Thok Fm	Reddish, eolian sandstone & siltstone	no fossils	Apt.–Tur.?
Phu Khat Fm	Reddish to whitish grey, sandstone & mudstone	no fossils	L. Cretaceous

42 *Palynological age estimations of the Khok Kruat and Maha Sarakham Formations are quoted by Sattayarak et al.
 43 (1991a,b). However, no palyno-fossil assemblage data were presented.

44

45

46 **Table S2:** Stratigraphic compilation of the climate-sensitive sediments with special emphasis
 47 on desert (eolian dune) deposits cited in **Figure 3**.

48

Locality No.	Basin	Formation	Lithology	Age	References
1	Gobi basin, Mongolia	Khukhteeg & Bayanshiree Fms	Whitish-grey, conglomerate, sandstone, mudstone, lignite, & Reddish-brown to whitish-grey, conglomerate, sandstone, mudstone	Alb. to Cen.-San.	Jerzykiewicz & Russell, 1991; Khand et al., 2000
2	Subei basin, China	Gecun & Pukou Fms	Reddish-orange to greenish-grey, sandstone, mudstone, & Reddish-purple to grey, pebbly sandstone	Apt.-Alb. to Cen.-Con.	Jiang & Li, 1996; Hao et al., 2000
3	Jiangnan basin, China	Wulong & Luojinghu Fms	Reddish to yellowish-grey, conglomerate, sandstone, mudstone & Reddish-purple to grey, conglomerate, sandstone	Alb. to Cen.-Tur.	Jiang & Li, 1996; Hao et al., 2000
4	Sichuan basin, China	Jiaguan Fm	Reddish-purple, fine- to medium-grained, <u>eolian sandstone</u>	Apt.-Tur.	Jiang et al., 2001
5	Simao basin, China	Nanxin & Bashahe Fms	Reddish-purple, sandstone, mudstone & Reddish-purple, <u>eolian sandstone</u> , sandy mudstone	Apt.-Alb. to Cen.-Tur.	Jiang et al., 2001
6	Khorat basin, Thailand	Maha Sarakhan & Phu Thok Fms	Reddish, sandstone, siltstone, salts, gypsums, & Reddish, <u>eolian sandstone</u> , siltstone	Apt.-Tur.?	Imsamut, 1996; Hasegawa et al., 2010
7	Iberian basin, Spain	Escucha & Utrillas Fms	Fine-grained <u>eolian sandstone</u> , siltstone, mudstone	Alb.-Cen.	Rodriguez-Lopez et al., 2006, 2008
8	British Columbia, Canada	Boulder Creek Fm	Grayish very fine-grained sandstone, Greenish-gray mudstone, sphaerosiderite-bearing paleosol	Alb.-Cen.	Leckie et al., 1989; Ufnar et al., 2005
9	North Alberta, Canada	Peace River Fm	Grayish sandstone, mudstone, sphaerosiderite-bearing paleosol	Alb.-Cen.	Ufnar et al., 2005
10	South Alberta, Canada	Mill Creek & Bow Island Fms	Reddish and grayish-greenish sandstone, pale yellow to dark red mudstone, paleosol	Alb.	McCarthy et al., 1997, 1999
11	Ontario basin, Canada	Mattagami Fm	Varicolored conglomerate, sandstone, mudstone, lignite	Apt.-Alb. to Cen.	White et al., 2000
12	Western Iowa basin	Dakota & Swan River Fms	Grayish sandstone, mudstone, sphaerosiderite-bearing paleosol	Alb.-Cen.	Ludvigson et al., 1998; White et al., 2000
13	Southwest Utah basin	Upper part of the Dakota Fm	Varicolored conglomerate, sandstone, mudstone, coal	Cen.-Tur.	Laurin & Sageman, 2007; Barclay et al., 2010
14	New Mexico basin	Sarten & Moreno Hill Fms	Reddish to pale yellowish sandstone, mudstone, paleosol	Alb.-Cen. to Tur.	Mack, 1992
15	Araripe basin, Brazil	Santana Fm	Sandstone, mudstone, black shale	Alb.	Heimhofer et al., 2008
16	Salta basin, Argentina	La Yesera Fm	Reddish-brown conglomerate, sandstone, siltstone, mudstone	Apt.-Alb.	Marquillas et al., 2005
17	Neuquen basin, Argentina	Lohan Cura Fm	Reddish-brown to greenish gray conglomerate, sandstone, siltstone, shale	Apt.-Alb.	Leanza et al., 2004

18	Orange basin, Namibia	Alb. to Cen. succession	Whitish conglomerate, sandstone, siltstone, mudstone	Alb.–Cen.	Stevenson & McMillan, 2004;
19	Tendaguru basin, Tanzania	Makonde Fm	Reddish to purple, conglomerate, fine- to medium-grained sandstone, siltstone, mudstone	Apt.–Alb.	Bussert et al., 2009
20	Saurashtra basin, India	Than & Wadhwan Fms	Grayish sandstone, mudstone, coal & Reddish conglomerate, sandstone, mudstone, limestone	E. Cretaceous	Aslam, 1992
21	Gippsland basin, Australia	Wonthaggi Fm	Volcanogenic sandstone, mudstone, coal	Apt.–Alb.	Douglas & Williams, 1982; Tosolini et al., 2002
22	Gobi basin, Mongolia	Djadokhta, Barungoyot, Dzunmod Fms	Reddish brown to whitish grey, <u>eolian sandstone</u> , sandy mudstone, calcrete	Camp.–Maas.	Jerzykiewicz & Russell, 1991; Hasegawa et al., in submitted
23	Ordos basin, China	Tagaimiao Fm	Red to orange, fine- to medium-grained, <u>eolian sandstone</u>	San.–Camp.	Jiang & Li, 1996; Hao et al., 2000
24	Tarim basin, China	Subashi Fm	Whitish-grey to reddish, medium to coarse-grained sandstone, mudstone	Camp.–Maas.	Jiang & Li, 1996; Hao et al., 2000
25	Subei basin, China	Chishan Fm	Reddish-purple to greenish-grey, sandstone, mudstone	San.–Maas.	Jiang & Li, 1996; Hao et al., 2000
26	Jiangnan basin, China	Paomagang Fm	Reddish to whitish grey, sandstone, mudstone	Camp.–Maas.	Jiang & Li, 1996; Hao et al., 2000
27	Sichuan basin, China	Guankou Fm	Red to purple, fine-grained sandstone, mudstone, gypsum	Con.–Maas.	Jiang et al., 2001
28	Simao basin, China	Mankuanhe Fm	Red to purple, sandy mudstone, mudstone	Con.–Maas.	Jiang et al., 2001
29	Khorat basin, Thailand	Phu Khat Fm	Reddish to whitish grey, sandstone, mudstone	L. Cretaceous	Hasegawa et al., 2010
30	South Alberta, Canada	Belly River & Willow Creek Fms	Reddish brown to whitish grey, conglomerate, sandstone, mudstone, calcrete	Camp.–Maas.	Jerzykiewicz & Sweet, 1988;
31	Western Montana basin, Canada	Two Medicine Fm	Reddish brown to whitish grey, conglomerate, sandstone, mudstone, calcrete	Camp.–Maas.	Lorenz, 1981
32	Eastern Montana basin, Canada	Hell Creek Fm	Varicolored conglomerate, sandstone, mudstone, coal	Maas.	Retallack, 1994; Johnson et al., 2002
33	North Dakota basin	Hell Creek Fm	Varicolored conglomerate, sandstone, mudstone, coal	Maas.	Fastovsky & mcSweeney, 1987 Johnson et al., 2002
34	Southwest Utah basin	Wahweap & Kaiparowits Fms	Varicolored conglomerate, sandstone, mudstone	Camp.–Maas.	Lawton et al., 2003
35	New Mexico basin	MacRae Fm	Reddish-brown to greyish, conglomerate, sandstone, mudstone, calcrete	Maas.	Buck & Mack, 1995
36	Western Texas basin	Aguja & Javelina Fms	Reddish purple to grayish, sandstone, mudstone, paleosol	Maas.	Lehman, 1989, 1990
37	Salta basin, Argentina	Lecho Fm	Whitish, fine- to medium-grained, <u>eolian sandstone</u>	Maas.	Marquillas et al., 2005
38	Bauru basin, Brazil	Rio Parana Fm, Caiua Gp.	Fine- to medium-grained, quartz <u>eolian sandstone</u>	Con.–Maas.	Fernandes et al., 2007

39	Parana basin, Brazil	Marilyn Fm	Medium- to coarse-grained, quartz-feldspar <u>eolian sandstone</u> , calcretes	Maas.	Goldberg & Garcia, 2000
40	Neuquen basin, Argentina	Anacleto & Allen Fms	Reddish to greenish-gray, conglomerate, sandstone, siltstone, mudstone	San.–Maas.	Leanza et al., 2004
41	Anambra basin, Namibia	Mamu & Ajali Fms	Conglomerate, sandstone, shale, coal	Camp.–Maas.	Tuttle, 1999
42	Congo basin, Angola	Nsele Gp	Medium- to coarse-grained sandstone, <u>eolian accumulation texture</u>	L.Cretaceous	Giresse, 2005
43	Orange basin, Namibia	Upper Santonian succession	Brownish sandstone, mudstone	L. Santonian	Stevenson & McMillan, 2004;
44	Dongargaonbasin, India	Lameta Fm	Reddish to greenish, conglomerate, sandstone, mudstone, calcrete	Maas.	Mohabey et al., 1993; Mohabey, 1996
45	Gippsland basin, Australia	Latrobe Gp.	Conglomerate, sandstone, mudstone, coal, volcanics	Camp.–Maas.	Wagstaff et al., 2006; Gallagher et al., 2008

49

50

51 **Supplementary Methods:**

52 *Paleoposition of eolian sandstone deposits in Asian interior basins*

53 Paleolatitude and rotation estimates of the studied basins, which are reconstructed based on
54 paleomagnetic data (Cheng et al., 1988; Zhuang, 1988; Otofujii et al., 1990; Enkin et al.,
55 1991; Zheng et al., 1991; Chen et al., 1993; Huang and Opdyke, 1993; Hankard et al., 2005;
56 Charusiri et al., 2006; **Fig. 1** and **Table 1**), are the critical basis for the present study which
57 demonstrate that the location of the subtropical high-pressure belt changed significantly
58 during the Cretaceous. Based on the obtained paleomagnetic data sets, paleolatitudes of the
59 North China block (Ordos Basin: N32.6°–41.0°; Cheng et al., 1988; Zheng et al., 1991) and
60 the South China block (Sichuan Basin: N25.5°–29.6°; Zhuang *et al.*, 1988; Enkin et al., 1991)
61 were different by more than 5° during the Cretaceous (**Fig. 1** and **Table 1**). The Gobi Basin of
62 southern Mongolia was located much higher latitude during the Cretaceous (N44.0°–46.1°;
63 Hankard et al., 2005). Reconstruction of the paleoposition of Indochina block during the
64 Cretaceous, prior to the India-Asia collision, has been controversial. For example, Chen *et al.*
65 (1992) argued that both Indochina block and South China block were located between N20°
66 and N30° during the Cretaceous, based on the paleomagnetic data reported by Yang and
67 Basse (1993). However, the paleomagnetic data reported by Yang and Basse (1993) is for the
68 upper Triassic to the lower Cretaceous deposits in the Khorat Basin (Indochina block) in
69 northeastern Thailand, and no paleomagnetic data of the mid- to upper Cretaceous deposits,
70 which contain eolian sandstone deposits in this area, was reported. On the other hand,
71 Charusiri et al. (2006) conducted the paleomagnetic study on the mid- to upper Cretaceous
72 deposits in the Khorat Basin, northeastern Thailand for the first time. They concluded that the
73 Khorat Basin was located between N16.3° and 21.6° during the mid- to late Cretaceous time
74 (Charusiri et al., 2006), which was much lower than that of South China block
75 (N25.5°–29.6°; Zhuang *et al.*, 1988; Enkin et al., 1991). Therefore, eolian sandstones were
76 distributed in ca. N30°–40° (Ordos and Tarim basins) during the early Cretaceous, shifted
77 southwards to ca. N20°–30° (Sichuan and Khorat basins) during the mid-Cretaceous, and
78 shifted northwards again to ca. N30°–45° (Gobi and Ordos basins) during the late Cretaceous,
79 implying that the significant latitudinal shifts of the distribution of eolian sandstone deposits
80 have occurred between the early, mid-, and late Cretaceous (**Fig. 1**).

81

82 *Age constraints for eolian sandstone formations in Asian interior basins*

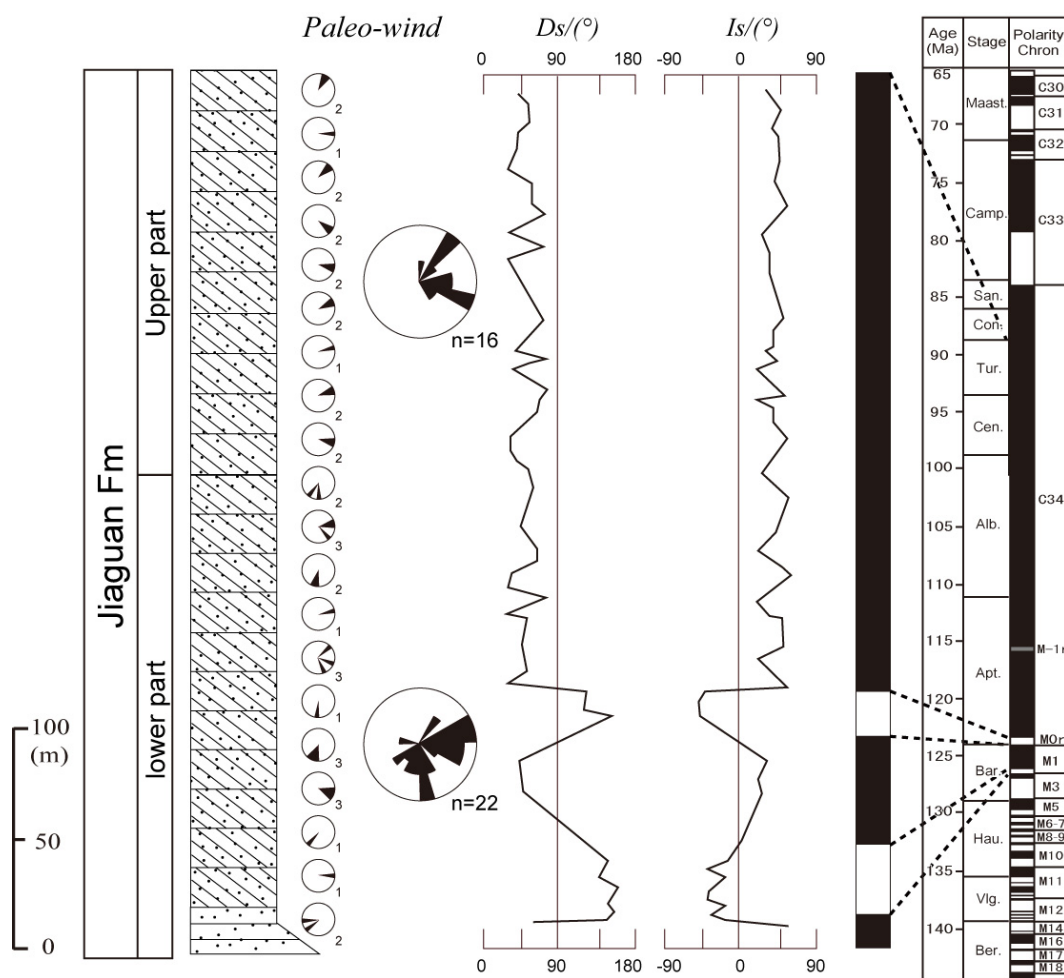
83 Although non-marine strata generally have chronostratigraphic uncertainties, our selected
84 data sets of eolian sandstone formations in the Asian interior basins have good age controls
85 based on magnetostratigraphy and/or biostratigraphy (Li, 1982; Jerzykiewicz and Russell,
86 1991; Jiang and Li, 1996; Racey et al., 1996; Hao et al., 2000; Khand et al., 2000; Meesok,
87 2000; Jiang et al., 2001; Chen et al., 2006; Sha, 2007; **Fig. 1** and **Table S1**), including the
88 results of our magnetostratigraphic studies (Imsamut, 1996; Pan et al., 2004; Hasegawa et al.,
89 2010; **Figs. S1, S2**). Paleontological age constraints provide a starting point for the ages of
90 the eolian sandstone formations cited in this study. A relatively rich record of fossil ostracods,
91 charophytes, plants, pollens, and spores has been collected from the studied sites (**Table S1**).
92 Particularly important are the ages of the eolian sandstone formations in Sichuan Basin and
93 Khorat Basin (the Jiaguan Formation and the Phu Thok Formation), because they provide the
94 critical time constraints on the low latitude desert distribution during the mid-Cretaceous.
95 The ages of these formations are well constrained by our magnetostratigraphic data (Imsamut,
96 1996; Pan et al., 2004; Hasegawa et al., 2010) in conjunction with paleontological age
97 constraints as described below.

98 The age of the Jiaguan Formation in Sichuan Basin is assigned to the Aptian–Turonian based
99 on the ostracod's biostratigraphy of the Jiaguan Formation, which yields age-diagnostic
100 ostracodes such as *Ziziphocypris orbita*, *Cypridea (Bisulcocypridea)* sp.
101 (Cenomanian–Turonian), and *Latonia (Monosulcocypris)* spp. (Aptian) (Li, 1982; Hao et al.,
102 2000; Chen et al., 2006; **Table S1**). Such age constraint is consistent with the ostracod's
103 biostratigraphy of the underlying Tianmashan Formation (Berriasian–Barremian) and
104 overlying Guankou Formation (Coniacian–Maastrichtian). In addition, the obtained
105 paleomagnetic polarity sequence of the Jiaguan Formation reveals short repetition of
106 reverse-normal-reverse polarity changes in its lowermost part and thick normal polarity zone
107 in its main part (Pan et al., 2004), which correlate best with chron M1r to superchron C34n of
108 the geomagnetic polarity time scale (GPTS; Gradstein et al., 2004). These results suggest that
109 deposition of the Jiaguan Formation began approximately at 127 Ma and ended no later than
110 ca. 84 Ma (from late Barremian–early Aptian to no later than late Santonian) (Pan et al.,
111 2004; **Fig. S1**).

112 Age constraints of the Phu Thok Formation in Khorat Basin are provided by the
113 palynological evidences of the underlying strata, the lignite-bearing Phra Wihan Formation,

114 which yields age-diagnostic palyno-fossils such as *Cicatricosisporites augustus* indicating
115 the age no older than Berriasian and *Dicheiropollis etruscus* indicating the age of Barremian
116 (Racey et al., 1996). Thus, age of the Phra Wihan Formation is assigned to the early
117 Cretaceous (Berriasian–Barremian), and the age of the overlying Phu Thok Formation is
118 younger than Barremian age (Racey et al., 1996; Meesok, 2000; DMR, 2001; Charusiri et al.,
119 2006; **Table S1**). Our newly established paleomagnetic polarity sequence of the Phu Thok
120 Formation reveals short repetition of reverse-normal-reverse polarity changes in its
121 lowermost part and thick normal polarity zone in its main part (Imsamut, 1996; Hasegawa et
122 al., 2010; **Fig. S2**), which can be correlated with chron M1n to superchron C34n of the GPTS
123 (Gradstein et al., 2004). Consequently, deposition of the Phu Thok Formation is interpreted
124 as having started approximately at 126 Ma and ended no younger than ca. 84 Ma (from late
125 Barremian–early Aptian to no younger than late Santonian), which is approximately the same
126 age as the Jiaguan Formation in Sichuan Basin. In summary, the low latitude deserts in Asia
127 emerged between late Barremian and early Aptian and disappeared between Turonian and
128 Coniacian according to the magnetostratigraphic correlations and paleontological age
129 constraints of the eolian sandstone formations in the Sichuan Basin (Jiaguan Formation) and
130 the Khorat Basin (Phu Thok Formation) given above (**Fig. 1**).

131

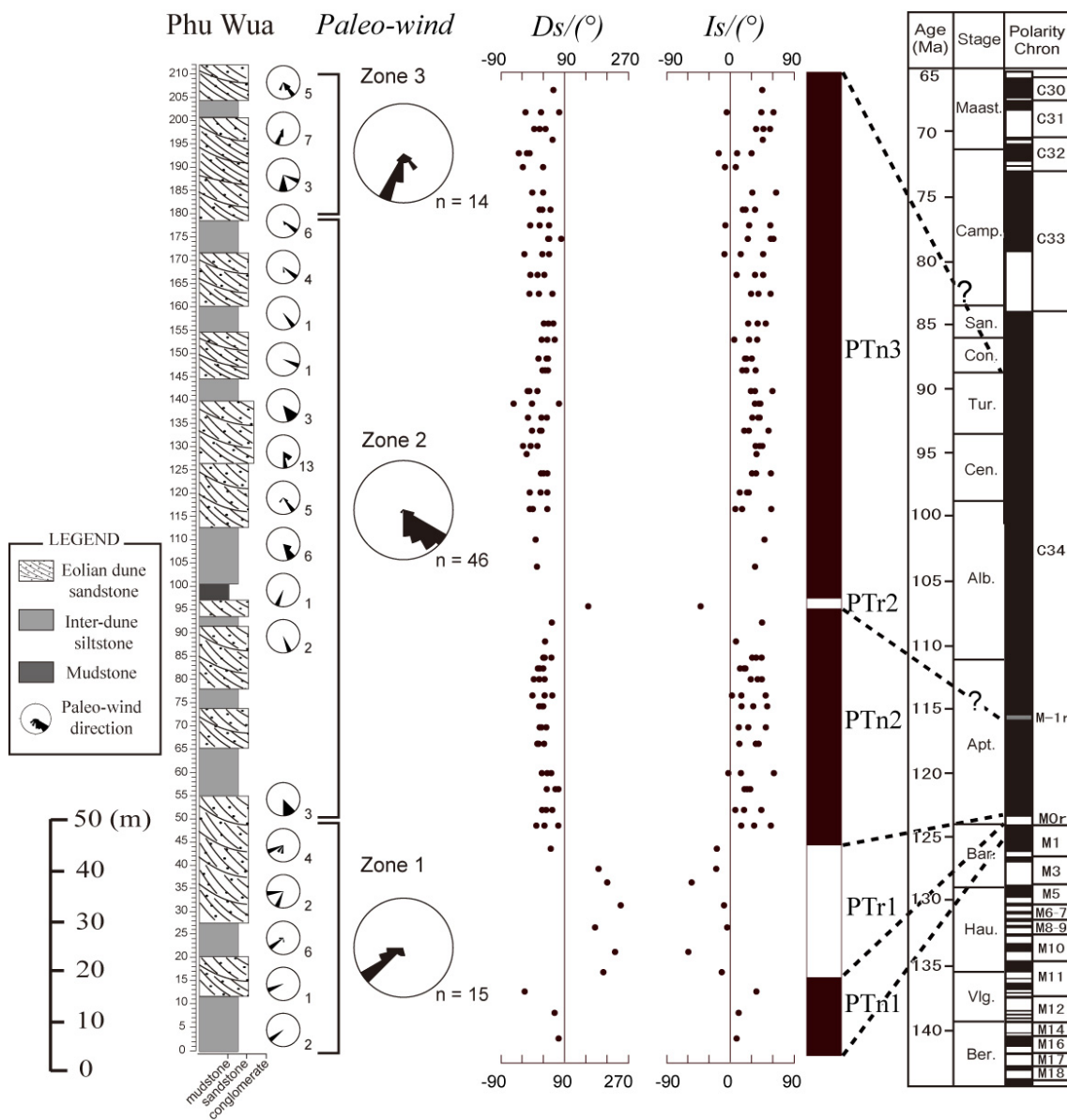


132

133 **Fig. S1:** Lithostratigraphic column, paleowind direction data, and magnetic polarity sequence
 134 of the eolian sandstone deposits (Jiaguan Formation) in Sichuan Basin, south China (Jiang et
 135 al., 1999; Pan et al., 2004; Hasegawa et al., 2010), and their correlation to the geomagnetic
 136 polarity time scale (GPTS) of the geological time scale 2004 (Gradstein et al., 2004).
 137 Magnetic polarity zones are shown by black and white bars for normal and reversed
 138 polarities.

139

140



141

142 **Fig. S2:** Lithostratigraphic column, paleowind direction data, and magnetic polarity sequence
 143 of the eolian sandstone deposits (Phu Thok Formation) in the Khorat Basin, northeast
 144 Thailand (Imsamut, 1996; Hasegawa et al., 2010), and their correlation to the GPTS
 145 (Gradstein et al., 2004). Magnetic polarity zones are shown by black (white) bars for normal
 146 (reversed) polarity.

147

148

149 **Supplementary References**

- 150 Aslam, M., 1992. Delta plain coal deposits from the Than Formation of the Early Cretaceous
151 Saurashtra basin, Gujarat, western India. *Sedimentary Geology* 81, 181–193.
- 152 Barclay, R.S., McElwain, J.C., Sageman, B.B., 2010. Carbon sequestration activated by a
153 volcanic CO₂ pulse during Ocean Anoxic Event 2. *Nature Geoscience* 3, 205–208.
- 154 Buck, B.J., Mack, G.H. 1995. Latest Cretaceous (Maastrichtian) aridity indicated by
155 paleosols in the McRae Formation, south-central New Mexico. *Cretaceous Research* 16,
156 559–572.
- 157 Bussert, R., Heinrich, W.D., Aberhan, M., 2009. The Tendaguru Formation (Late Jurassic to
158 Early Cretaceous, southern Tanzania): definition, palaeoenvironments, and sequence
159 stratigraphy. *Fossil Record* 12, 141–174.
- 160 Douglas, J.G., Williams, G.E., 1982. Southern polar forests: The Early Cretaceous floras of
161 Victoria and their palaeoclimatic significance. *Palaeogeography, Palaeoclimatology,*
162 *Palaeoecology* 39, 171–185.
- 163 Fastovsky, D.E., McSweeney, K., 1987. Paleosols spanning the Cretaceous-Paleogene
164 transition, eastern Montana and western North Dakota. *Geological Society of America*
165 *Bulletin* 99, 66–77.
- 166 Gallagher, S.J., et al., 2008. Southern high latitude climate variability in the Late Cretaceous
167 greenhouse world. *Global and Planetary Change* 60, 351–364.
- 168 Hasegawa, H., Suganuma, Y., Seike, K., Tada, R., Ichinnorov, N., Badamgarav, D., Khand, Y.,
169 in submitted. Magnetostratigraphy and depositional environments of Upper Cretaceous
170 deposits in the Gobi Basin, southern Mongolia: implications for desert development in
171 mid-latitude Asia. (in submitted to *Journal of Asian Earth Sciences*)
- 172 Heimhofer, U., et al., 2008. Evidence for photic-zone euxinia in the Early Albian Santana

- 173 Formation (Araripe Basin, NE Brazil). *Terra Nova* 20, 347–354.
- 174 Jerzykiewicz, T., Sweet, A.R., 1988. Sedimentological and palynological evidence of
175 regional climatic changes in the Campanian to Paleocene sediments of the Rocky
176 Mountain Foothills, Canada. *Sedimentary Geology* 59, 29–76.
- 177 Jiang, X.S., Pan, Z.X., Fu, Q.P., 1999. The variations of palaeowind direction of the
178 Cretaceous desert in the Sichuan Basin and their significance. *Sedimentary Facies and*
179 *Palaeogeography* 19, 1–11.
- 180 Johnson, K.R., Nichols, D.J., Hartman, J.H., 2002. Hell Creek Formation: A 2001 synthesis.
181 Geological Society of America Special Paper 361, 503–510.
- 182 Laurin, J., Sageman, B., 2007. Cenomanian_Turonian coastal record in SW Utah, USA:
183 Orbital scale transgressive-regressive events during Oceanic Anoxic Event II. *Journal*
184 *of Sedimentary Research* 77, 731–756.
- 185 Lawton, T.F., Polloch, S.L., Robinson, R.A.J., 2003. Integrating sandstone petrology and
186 nonmarine sequence stratigraphy: Application to the late cretaceous fluvial systems of
187 southwestern Utah, USA. *Journal of Sedimentary Research* 73, 389–406.
- 188 Leanza, H.A., Apesteguía, A., Novas, F.E., de la Fuente, M.S., 2004. Cretaceous terrestrial
189 beds from the Neuquén Basin (Argentina) and their tetrapod assemblages. *Cretaceous*
190 *Research* 25, 61–87.
- 191 Leckie, D., Fox, C., and Tarnocai, C., 1989. Multiple paleosols of the late Albian Boulder
192 Creek Formation, British Columbia, Canada: *Sedimentology* 36, 307–323.
- 193 Lehman, T.M., 1989. Upper Cretaceous (Maastrichtian) Paleosols in Trans-Pecos Texas.
194 Geological Society of America Bulletin 101, 188–203.
- 195 Lehman, T.M., 1990. Paleosols and the Cretaceous/Tertiary transition in the Big Bend region
196 of Texas. *Geology* 18, 362–364.

197 Lorenz, J.C., 1981. Sedimentary and tectonic history of the Two Medicine Formation, Late
198 Cretaceous (Campanian), northwestern Montana. Ph.D. Thesis, Princeton University,
199 Princeton, N.J., pp.214 .

200 Mack, G.H., 1992. Paleosols as an indicator of climatic-change at the early-late Cretaceous
201 boundary, Southwestern New Mexico. *Journal of Sedimentary Petrology* 62, 483–494.

202 McCarthy, P.J., Martini, I.P., Leckie, D.A., 1997. Anatomy and evolution of a Lower
203 Cretaceous alluvial plain: Sedimentology and palaeosols in the upper Blairmore Group,
204 south-western Alberta, Canada. *Sedimentology* 44, 197–220.

205 McCarthy, P.J., Martini, I.P., Leckie, D.A., 1999. Pedogenic and diagenetic influences on
206 void coating formation in Lower Cretaceous paleosols of the Mill Creek Formation,
207 southwestern Alberta, Canada. *Geoderma* 87, 209–237.

208 Mohabey, D.M., Udhoji, S.G., Verma, K.K., 1993. Palaeontological and sedimentological
209 observations on non-marine Lameta Formation (Upper Cretaceous) of Maharashtra,
210 India: their palaeoecological and palaeoenvironmental significance. *Palaeogeography,*
211 *Palaeoclimatology, Palaeoecology* 105, 83–94.

212 Mohabey, D.M., 1996. A new oospecies, *Megaloolithus matleyi*, from the Lameta Formation
213 (Upper Cretaceous) of Chandrapur district, Maharashtra, India, and general remarks on
214 the palaeoenvironment and nesting behaviour of dinosaurs. *Cretaceous Research* 17,
215 183–196.

216 Retallack, G.J., 1994. A pedotype approach to latest Cretaceous and earliest Tertiary paleosols
217 in eastern Montana. *Geological Society of America Bulletin* 106, 1377–1397.

218 Rodriguez-Lopez, J.P., de Boer, P.L., Melendez, N., Soria, A.R., Pardo, G., 2006.
219 Windblown desert sands in coeval shallow marine deposits: a key for the recognition of
220 coastal ergs in the mid-Cretaceous Iberian Basin, Spain. *Terra Nova* 18, 314–320.

221 Rodriguez-Lopez, J.P., Melendez, N., de Boer, P.L., Soria, A.R., 2008. Aeolian sand sea
222 development along the mid-Cretaceous western Tethyan margin (Spain): erg
223 sedimentology and palaeoclimate implications. *Sedimentology* 55, 1253–1292.

224 Sattayarak, N., Srigulwong, S., Patarametha, M., 1991a. Subsurface stratigraphy of the
225 non-marine Mesozoic Khorat Group, Northern Thailand. *GEOSEA VII*, Bangkok, 36A.

226 Sattayarak, N., Polachan, S., Charusirisawad, R., 1991b. Cretaceous rock salt in the
227 northeastern part of Thailand. *GEOSEA VII*, Bangkok, 36A.

228 Stevenson, I.R., McMillan, I.K., 2004. Incised valley fill stratigraphy of the Upper
229 Cretaceous succession, proximal Orange Basin, Atlantic margin of southern Africa.
230 *Journal of the Geological Society, London* 161, 185–208.

231 Tosolini, A.M.P., McLoughlin, S., Drinnan, A.N., 2002. Early Cretaceous megaspore
232 assemblages from southeastern Australia. *Cretaceous Research* 23, 807–844.

233 Tuttle, M.L.W., Charpentier, R.R., Brownfield, M.E., 1999. The Niger Delta Petroleum
234 System: Niger Delta Province, Nigeria, Cameroon, and Equatorial Guinea, Africa.
235 Open-File Report, U.S. Department of the Interior, U.S. Geological Survey, pp.64.

236 Ufnar, D.F., et al., 2005. Reconstructing a mid-Cretaceous landscape from paleosols in
237 western Canada. *Journal of Sedimentary Research* 75, 984–996.

238 Wagstaff, B.E., Gallagher S.J., Lanigan, K.P., 2006. Late Cretaceous palynological
239 correlation and environmental analysis of fluvial reservoir facies of the Tuna Field,
240 Gippsland Basin, southeast Australia. *Review of Palaeobotany and Palynology* 138,
241 165–186.

242 White, T.S., Witzke, B., Ludvigson, G., 2000. Evidence for an Albian Hudson Arm of the
243 North American Cretaceous Western Interior Seaway. *Geological Society of America*
244 *Bulletin* 112, 1342–1355.